



Gamma-Aminobutyric Acid Signaling in Brown Adipose Tissue Promotes Systemic Metabolic Derangement in Obesity

Ikegami, Ryutaro; Shimizu, Ippei; Sato, Takeshi; Yoshida, Yohko; Hayashi, Yuka; Suda, Masayoshi; Katsuumi, Goro; Li, Ji; Wakasugi, Takayuki; Minokoshi, Yasuhiko; Okamoto, Shiki; Hinoi, Eiichi; Nielsen, Søren; Jespersen, Naja Zenius; Scheele, Camilla; Soga, Tomoyoshi; Minamino, Tohru

Published in:
Cell Reports

DOI:
[10.1016/j.celrep.2018.08.024](https://doi.org/10.1016/j.celrep.2018.08.024)

Publication date:
2018

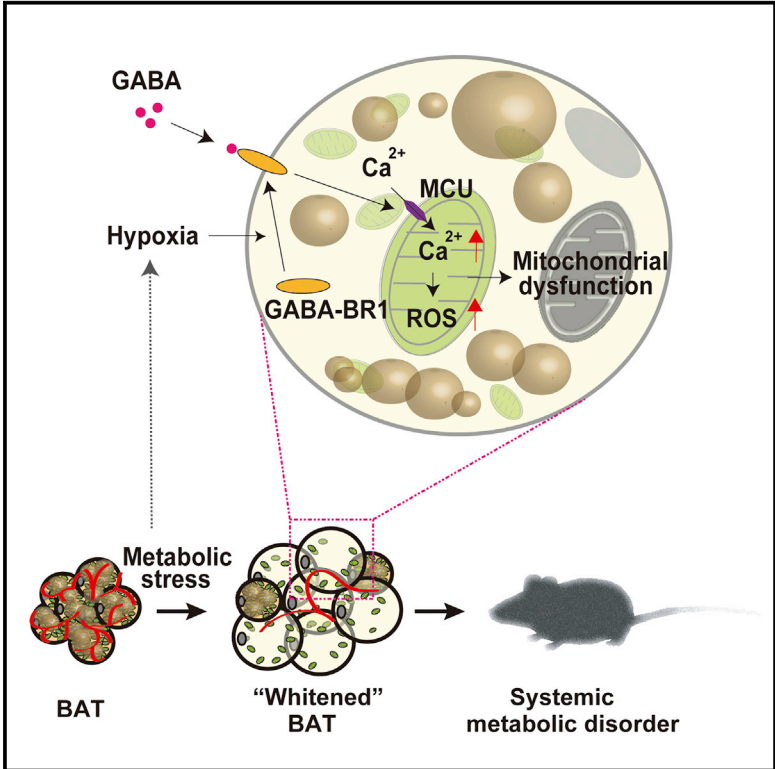
Document version
Publisher's PDF, also known as Version of record

Document license:
[CC BY-NC-ND](https://creativecommons.org/licenses/by-nc-nd/4.0/)

Citation for published version (APA):
Ikegami, R., Shimizu, I., Sato, T., Yoshida, Y., Hayashi, Y., Suda, M., ... Minamino, T. (2018). Gamma-Aminobutyric Acid Signaling in Brown Adipose Tissue Promotes Systemic Metabolic Derangement in Obesity. *Cell Reports*, 24(11), 2827-2837.e5. <https://doi.org/10.1016/j.celrep.2018.08.024>

Gamma-Aminobutyric Acid Signaling in Brown Adipose Tissue Promotes Systemic Metabolic Derangement in Obesity

Graphical Abstract



Authors

Ryutaro Ikegami, Ipppei Shimizu, Takeshi Sato, ..., Camilla Scheele, Tomoyoshi Soga, Tohru Minamino

Correspondence

ippeishimizu@yahoo.co.jp (I.S.), tminamino@med.niigata-u.ac.jp (T.M.)

In Brief

Brown adipose tissue (BAT) is a metabolically active organ important for systemic metabolism. Here, Ikegami et al. identify a role for gamma-aminobutyric acid (GABA) in metabolic and BAT dysfunction in obese mice and demonstrate that inhibition of GABA/GABA-BR1-mediated signaling and of mitochondrial calcium overload can restore BAT function in obesity.

Highlights

- GABA and GABA-BR1 are increased in brown adipose tissue (BAT) in obesity
- GABA signaling promotes BAT and mitochondrial dysfunction in obese mice
- GABA-BR1 inhibition ameliorates BAT dysfunction and promotes BAT re-browning
- Inhibition of GABA signaling and mitochondrial calcium overload restore BAT function



Gamma-Aminobutyric Acid Signaling in Brown Adipose Tissue Promotes Systemic Metabolic Derangement in Obesity

Ryutaro Ikegami,^{1,8} Ippei Shimizu,^{1,2,8,*} Takeshi Sato,^{1,8} Yohko Yoshida,^{1,2} Yuka Hayashi,¹ Masayoshi Suda,¹ Goro Katsumi,¹ Ji Li,¹ Takayuki Wakasugi,¹ Yasuhiko Minokoshi,³ Shiki Okamoto,³ Eiichi Hinoi,⁴ Søren Nielsen,⁵ Naja Zenius Jespersen,⁵ Camilla Scheele,^{5,6} Tomoyoshi Soga,⁷ and Tohru Minamino^{1,9,*}

¹Department of Cardiovascular Biology and Medicine, Niigata University Graduate School of Medical and Dental Sciences, Niigata 951-8510, Japan

²Division of Molecular Aging and Cell Biology, Niigata University Graduate School of Medical and Dental Sciences, Niigata 951-8510, Japan

³Department of Homeostatic Regulation, Division of Endocrinology and Metabolism, National Institute for Physiological Sciences, National Institutes of Natural Sciences, Aichi 444-8585, Japan

⁴Department of Molecular Pharmacology, Faculty of Pharmaceutical Sciences, Kanazawa University, Ishikawa 920-1192, Japan

⁵The Centre of Inflammation and Metabolism and Centre for Physical Activity Research Rigshospitalet, Copenhagen, Denmark

⁶Novo Nordisk Foundation Center for Basic Metabolic Research, University of Copenhagen, Copenhagen, Denmark

⁷Institute for Advanced Biosciences, Keio University, Yamagata 997-0052, Japan

⁸These authors contributed equally

⁹Lead Contact

*Correspondence: ippeishimizu@yahoo.co.jp (I.S.), tminamino@med.niigata-u.ac.jp (T.M.)

<https://doi.org/10.1016/j.celrep.2018.08.024>

SUMMARY

Brown adipose tissue (BAT) is a metabolically active organ that contributes to the maintenance of systemic metabolism. The sympathetic nervous system plays important roles in the homeostasis of BAT and promotes its browning and activation. However, the role of other neurotransmitters in BAT homeostasis remains largely unknown. Our metabolomic analyses reveal that gamma-aminobutyric acid (GABA) levels are increased in the interscapular BAT of mice with dietary obesity. We also found a significant increase in GABA-type B receptor subunit 1 (GABA-*BR1*) in the cell membranes of brown adipocytes of dietary obese mice. When administered to obese mice, GABA induces BAT dysfunction together with systemic metabolic disorder. Conversely, the genetic inactivation or inhibition of GABA-*BR1* leads to the re-browning of BAT under conditions of metabolic stress and ameliorated systemic glucose intolerance. These results indicate that the constitutive activation of GABA/GABA-*BR1* signaling in obesity promotes BAT dysfunction and systemic metabolic derangement.

INTRODUCTION

The worldwide prevalence of obesity remains high, and new therapies to treat obesity-related pathologies are urgently needed (NCD Risk Factor Collaboration (NCD-RisC), 2017). Brown adipose tissue (BAT) was initially characterized as a thermogenic organ in small rodents and human infants (Dawkins and Scopes, 1965; Smith and Roberts, 1964). However, it has been

recently reported that adult humans also possess functional BAT, and studies have shown that it is a metabolically active organ with the potential to regulate systemic metabolism (Bartelt et al., 2011; Jespersen et al., 2013; Stanford et al., 2013). Metabolic stress is reported to promote the whitening of BAT, which is associated with its dysfunction and with the development of systemic metabolic derangement (Shimizu et al., 2014). The conversion of white adipose tissue (WAT) to thermogenic brown adipose (commonly called “browning”) continues to be an important focus of research (Harms and Seale, 2013; Shinoda et al., 2015), along with the search for mechanisms that can suppress the “whitening” of BAT and its functional decline, in relation to the exploration of next-generation therapies for obesity and diabetes (Shimizu and Walsh, 2015).

The sympathetic nervous system and adrenergic signaling are critically important for the activation of BAT and for maintaining its homeostasis (Harms and Seale, 2013). The inhibition of peripheral serotonin synthesis has recently been shown to promote BAT thermogenesis, reduce obesity, and ameliorate systemic metabolic dysfunction (Crane et al., 2015). However, the role of other neurotransmitters in BAT is largely unknown. Gamma-aminobutyric acid (GABA) is the best characterized inhibitory neurotransmitter in the brain and mainly mediates its biological effects by suppressing neuronal excitability (Ko et al., 2015). There is evidence that GABA in the CNS is involved in the regulation of systemic metabolism. For example, the activation of GABA_A-receptor-mediated signaling in the lateral hypothalamus suppresses food intake and reduces body weight, and suppression of this signaling pathway promotes eating (Turenius et al., 2009). Agouti-related peptide (AgRP) and neuropeptide Y (NPY) neurons stimulate eating and are mostly GABAergic, and the genetic inactivation of GABA transporter expression in AgRP neurons results in a lean phenotype (Tong et al., 2008). The anti-obesity effect of leptin was reported to be mediated by the synaptic release of GABA from hypothalamic GABAergic neurons that



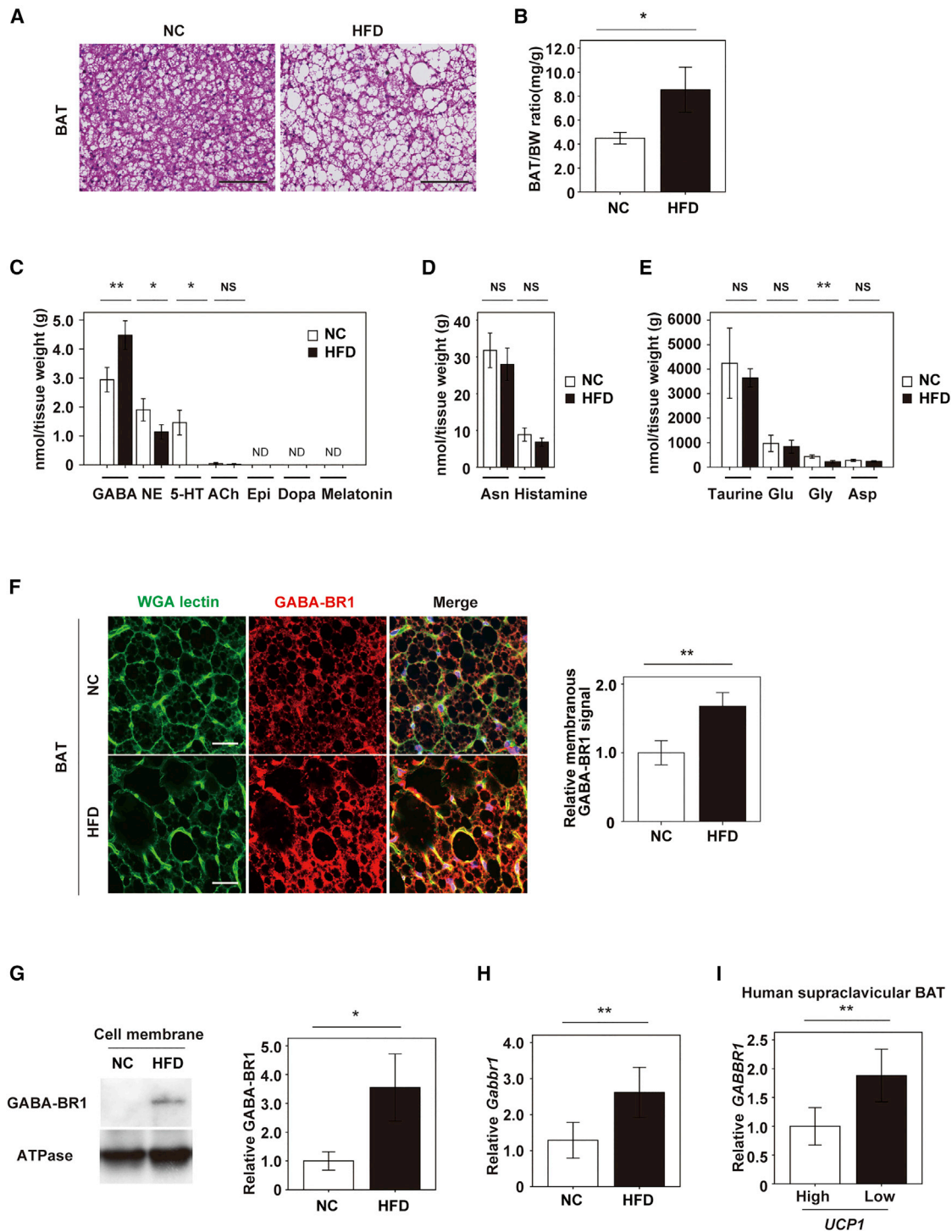


Figure 1. Evidence that GABA and GABA-BR1 Signals Are Increased in BAT under a Metabolic Stress

(A and B) H&E staining (A) and body weight (BW)-adjusted weight (B) of brown adipose tissue (BAT) from wild-type mice fed normal chow (NC) or a high-fat diet (HFD) (n = 4 and 4). In the HFD group, mice were fed the diet from 4 weeks of age and analyzed at 17 weeks of age. The scale bars represent 100 μ m. (C–E) BAT of wild-type mice with dietary obesity was subjected to metabolomic analyses with capillary electrophoresis-mass spectrometry (CE-MS) (n = 5 each). These mice were fed the HFD from 4 weeks of age and analyzed at 12 weeks of age. ND, not detected. GABA, gamma-aminobutyric acid; NE, norepinephrine; 5-HT, serotonin; ACh, acetylcholine; Epi, epinephrine; Dopa, dopamine; Melatonin (C), Asn, asparagine; Histamine (D) and Taurine; Glu, glutamic acid; Gly, glycine; Asp, aspartic acid (E).

(legend continued on next page)

also express leptin receptors, and suppression of this system leads to overeating and obesity (Xu et al., 2012). GABA is also detected in various peripheral organs, including the pancreas, endothelium, gastrointestinal tract, adrenal medulla, and placenta (Gladkevich et al., 2006; Sen et al., 2016). In patients with diabetes, GABA is reportedly decreased in the pancreas (Al-Salam et al., 2009). GABA promotes insulin secretion from the pancreas in normal rats, and this response is suppressed in the diabetic state (Adeghate and Ponery, 2002). Recently, GABA_A-receptor-mediated signaling was shown to promote the transformation of α cells to functional β -like cells in pancreatic islets, thereby contributing to the suppression of pathological changes linked to diabetes (Li et al., 2017). In contrast to the known effects of GABA in the CNS, its peripheral role is yet to be defined.

Here, we report a metabolomic analysis that identified several representative neurotransmitters in the interscapular BAT of mice, among which only GABA showed an increase in response to obesity and metabolic stress. Our *in vivo* and *in vitro* findings show that GABA/GABA-BR1 signaling promotes BAT dysfunction and contributes to the development of systemic metabolic derangement in obesity.

RESULTS

GABA and GABA-BR1 Are Increased in BAT under Obese Conditions

We generated a mouse model of dietary obesity by maintaining C57BL/6Ncr mice on a high-fat diet (HFD) (Figure S1A). This diet promoted the whitening of interscapular BAT and was associated with increased weight of this tissue, as reported previously (Figures 1A, 1B, and S1B; Shimizu et al., 2014). Adrenergic signaling is well known to have a central role in maintaining BAT homeostasis by promoting its browning and activation, but the influence of other neurotransmitters is largely unknown, especially with regard to the response to stress.

To address this question, we performed metabolomic analyses of interscapular BAT from mice using capillary electrophoresis-mass spectrometry (CE-MS). This analysis showed that norepinephrine levels were reduced in interscapular BAT by metabolic stress (Figure 1C). Among the neurotransmitters identified in this analysis, GABA was the only one to be increased in the interscapular BAT of mice with dietary obesity (Figures 1C–1E). GABA has been extensively studied in the CNS, but its role in adipose tissue is mostly unknown; we therefore further

characterized the influence of GABA in BAT. Immunofluorescence showed that GABA immunoreactivity was increased in interscapular BAT from obese mice (Figure S1C). We also found that metabolic stress increased GABA type B receptor subunit 1 (GABA-BR1) expression in the cell membranes of brown adipocytes *in vivo* (Figures 1F and 1G). GABA-BR1 (*Gabbr1*) transcripts were significantly increased in whole-tissue lysates of BAT from HFD-fed mice under metabolic stress (Figure 1H). Next, we analyzed GABA-BR1 levels in supraclavicular BAT samples obtained from 19 human volunteers (BMI = 18–31). Initially, they were divided into *UCP1* high and *UCP1* low groups, as described by Jespersen et al. (2013). Uncoupling protein 1 (*UCP-1*) is a mitochondrial protein responsible for thermogenic respiration (Nedergaard et al., 2001). When the *GABBR1* levels of the high and low *UCP1* groups were compared, we found *GABBR1* levels to be significantly higher in individuals with low *UCP1* expression (Figure 1I). These results indicated that GABA/GABA-BR1 signaling might have biological effects on brown adipocytes in rodents and humans, especially in the presence of obesity.

The next issue we addressed was the origin of increased GABA in BAT associated with obesity. Our metabolomic analysis showed that circulating GABA levels do not increase with obesity (Figure S1D). In addition, the denervation of the sympathetic supply to interscapular BAT reduced norepinephrine to undetectable levels in BAT from both lean and obese groups (Figure S1E) but had little effect on GABA levels (Figure S1F). These findings suggest that GABA in BAT mainly derives from non-sympathetic nerves. We also investigated whether GABA was generated from glutamate by the GABA shunt in brown adipocytes. It has been reported that GABA is generated from glutamate by glutamate decarboxylase in pancreatic β cells (Li et al., 2013; Prentki et al., 2013), and this pathway also exists in the brain (Patel et al., 2005). In lean wild-type (WT) mice and mice with dietary obesity, glutamate decarboxylase protein was detected in the brain, but not in the BAT (Figure S1G). In addition, transcripts for glutamate decarboxylase 1 (*Gad1*) or glutamate decarboxylase 2 (*Gad2*) were detected in the brain, but not in the BAT of either lean WT mice or mice with dietary obesity, and transcripts were also not detected in differentiated brown adipocytes *in vitro* (Figures S1H and S1I). However, low expression of *Gad1* (but not *Gad2*) transcripts was detected in CD45⁺ cells extracted from the BAT of WT mice with dietary obesity (Figures S1J and S1K), indicating that CD45⁺ immune cells might make a minor contribution to GABA production in BAT under metabolic stress.

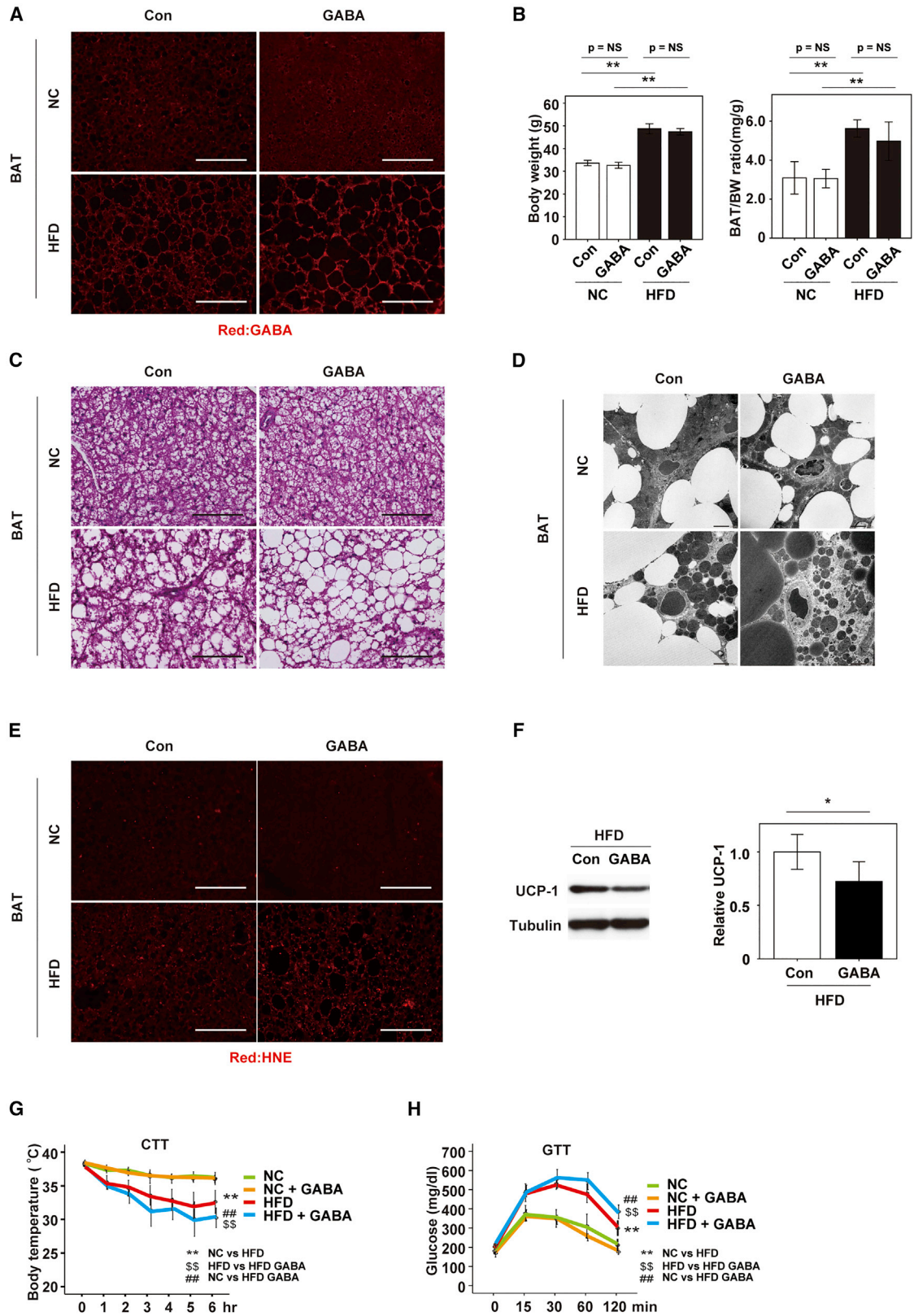
(F) Immunofluorescent staining for gamma-aminobutyric acid type B receptor subunit 1 (GABA-BR1) (red; scale bars = 20 μ m) in BAT of 17-week-old mice with dietary obesity (HFD) that were generated as described above. Nuclei and plasma membranes were stained with Hoechst (blue) and wheat germ agglutinin (WGA) lectin (green). The right panel shows quantification of the data (n = 4 and 4).

(G) Western blot analysis of GABA-BR1 in the cell membranes of BAT from wild-type mice fed NC or a HFD. Right panel displays quantification of GABA-BR1 relative to the ATPase loading control (n = 3 and 3).

(H) Transcripts for GABA-BR1 (*Gabbr1*) in BAT of mice (24–28 weeks old) fed NC or a HFD were evaluated by qPCR (n = 17 and 14).

(I) Transcripts for *GABBR1* in human supraclavicular BAT.

Samples obtained from 19 individuals were studied. Initially, data were divided into high *UCP1* and low *UCP1* groups, as described by Jespersen et al. (2013). *GABBR1* levels were compared between the high and low *UCP1* groups (n = 9 and 10). Results were normalized for *PPIA*. All data were analyzed by the two-tailed Student's t test. *p < 0.05; **p < 0.01. Values represent the mean \pm SEM. NS, not significant. Data are from one independent series of experiment (A, B, C–E, and G) from one of three independent series of experiments (F) or from three independent series of experiments (H). All data are from different biological replicates.



(legend on next page)

GABA Promotes BAT Dysfunction

To further investigate the role of GABA signaling in BAT, we added GABA to the drinking water of mice with dietary obesity. The oral intake of GABA reportedly does not increase GABA levels in the brain because GABA is unable to cross the blood brain barrier, especially in rodents (Boonstra et al., 2015), which our findings confirmed (Figure S2A), but it did markedly increase GABA in the interscapular BAT of obese mice (Figures 2A and S2B). The oral administration of GABA did not lead to increased food intake, body weight, or interscapular BAT weight (Figures 2B and S2C), but it promoted the whitening of interscapular BAT in mice with dietary obesity (Figures 2C and S2D). Electron microscopy showed that GABA administration led to mitochondrial fragmentation and rarefaction in interscapular BAT (Figure 2D) and also increased the levels of reactive oxygen species (ROS) (Figures 2E, S2E, and S2F). GABA administration also decreased mitochondrial brown fat UCP-1 levels in the interscapular BAT of obese mice at both protein and transcriptional levels (Figures 2F and S2G). There was also a reduced thermogenic response to metabolic stress and worsening of systemic glucose intolerance in obese mice administered GABA (Figures 2G and 2H). *In vitro*, the addition of GABA to cultures of differentiated brown adipocytes led to a significant reduction in transcripts that are associated with functional BAT, including *Ucp1*, *Mtnd5*, *Ppargc1a*, and *Ndufa1* (Figure S2H). Taken together, these *in vivo* and *in vitro* findings indicated that excessive GABA signaling promotes BAT dysfunction and systemic glucose intolerance in obese mice.

Suppression of GABA-BR1 Ameliorates BAT Dysfunction

Next, we analyzed a heterozygous knockout GABA-BR1 (*Gabbr1* KO) model generated in BALB/c mice (Schuler et al., 2001). Homozygous *Gabbr1*-null mice are reported to have epilepsy (Schuler et al., 2001); we therefore used heterozygous *Gabbr1* mice in our study. *Gabbr1* KO mice fed a HFD had a similar body weight and BAT weight to their WT littermates at 18 weeks of age (Figures S3A and S3B); by 55 weeks of age, the body weights of *Gabbr1* KO and WT mice still did not significantly differ (data not shown). The whitening of BAT associated with obesity was also ameliorated in *Gabbr1* KO mice (Figure 3A), and electron microscopy indicated that mitochondrial fragmen-

tation and rarefaction in brown adipocytes from interscapular BAT were both reduced (Figure 3B). Moreover, in *Gabbr1* KO mice, the levels of ROS in BAT were significantly reduced (Figures 3C and S3C), systemic glucose intolerance in the presence of metabolic stress was ameliorated (Figure 3D), and *Ucp1* expression in interscapular BAT was increased (Figure 3E).

To investigate a potential role for the sympathetic nervous system in this genetic model, we measured norepinephrine levels in interscapular BAT and found them to be similar in WT and *Gabbr1* KO mice (Figure S3D). To obtain more direct evidence of the beneficial effect of suppressing GABA/GABA-BR1 signaling for maintaining BAT function, we infused SCH-50911, a selective GABA-B receptor antagonist (GABA-BR blocker), around the interscapular BAT of WT mice for 2 weeks via an infusion pump. The administration of this GABA-BR blocker did not alter either the body weight or interscapular BAT weight of WT mice (Figures S3E and S3F). However, it contributed to the re-browning of BAT under metabolic stress (Figures 3F and S3G), reduced mitochondrial fragmentation and rarefaction in brown adipocytes (Figure 3G), and reduced the tissue ROS levels in BAT, relative to untreated controls (Figures 3H and S3H). The GABA-BR blocker also improved systemic glucose intolerance (Figure 3I) and the thermogenic response to the acute cold tolerance test (Figure S3I) in mice with dietary obesity. Furthermore, *Ucp1* levels in interscapular BAT were increased by administration of this compound (Figure 3J). Moreover, *in vitro*, the addition of SCH-50911 to cultures of differentiated brown adipocytes suppressed the GABA-induced mitochondrial production of ROS (Figure S3J) and prevented reduction of the mitochondrial membrane potential (Figure S3K).

To investigate the potential effects of the GABA-BR blocker on systemic metabolism and to further test our hypothesis that GABA-BR1 suppression contributes to the re-browning of whitened BAT under metabolic stress, we injected adeno-associated virus that encodes short hairpin RNA for *Gabbr1* (adeno-associated virus [AAV]-U6-GFP sh-*Gabbr1* [AAV sh-*Gabbr1*]) directly into the interscapular BAT of WT mice under direct visual guidance. Using the IVIS imaging system, we confirmed that AAV sh-*Gabbr1* was successfully delivered into the interscapular BAT and confirmed with qPCR analysis that *Gabbr1* transcripts were significantly reduced following this procedure (Figures S4A and S4B). We also analyzed *Gabbr1* levels in the liver, gonadal

Figure 2. GABA Promotes Dysfunction of Brown Adipose Tissue and Systemic Metabolic Derangement

Wild-type mice were fed NC or a HFD. In the HFD group, mice were fed the diet from 4 weeks of age and analyzed at 13–20 weeks of age. In some NC and HFD groups, GABA was mixed into the drinking water from 4 weeks of age (GABA).

(A) Immunofluorescent staining for GABA (red) in BAT of the indicated groups. The scale bars represent 100 μ m.

(B) Body weight (n = 7, 9, 9, and 11) and BAT weight adjusted by body weight (n = 7, 9, 9, and 11) were measured.

(C–E) Findings on H&E staining (C; scale bars = 100 μ m), transmission electron microscopy (D; scale bars = 2 μ m), and 4-hydroxy-2-nonenal (4-HNE) staining (E) of BAT (scale bars = 100 μ m).

(F) Western blot analysis of UCP-1 in BAT from wild-type mice fed a HFD with or without GABA administration. Right panel displays quantification of UCP-1 relative to the tubulin loading control (n = 8 and 8).

(G) Results of the acute cold tolerance test (n = 8, 6, 16, and 17).

(H) Results of glucose tolerance test (n = 9, 8, 14, and 14).

Data were analyzed by the two-tailed Student's t test (F) with non-parametric Kruskal-Wallis test (B; left panel [BW]) or two-way ANOVA followed by Tukey's multiple comparison test (B; right panel [BAT/BW ratio]; G and H). *p < 0.05; **p < 0.01 (B and F). **p < 0.01 NC versus HFD; \$\$\$p < 0.01 HFD versus HFD GABA; ###p < 0.01 NC versus HFD GABA (G and H). Values represent the mean \pm SEM. Data are from one of two independent series of experiments (A, C, and E) from two independent series of experiments (B and F), one independent series of experiment (D), or from three independent series of experiments (G and H). All data are from different biological replicates.

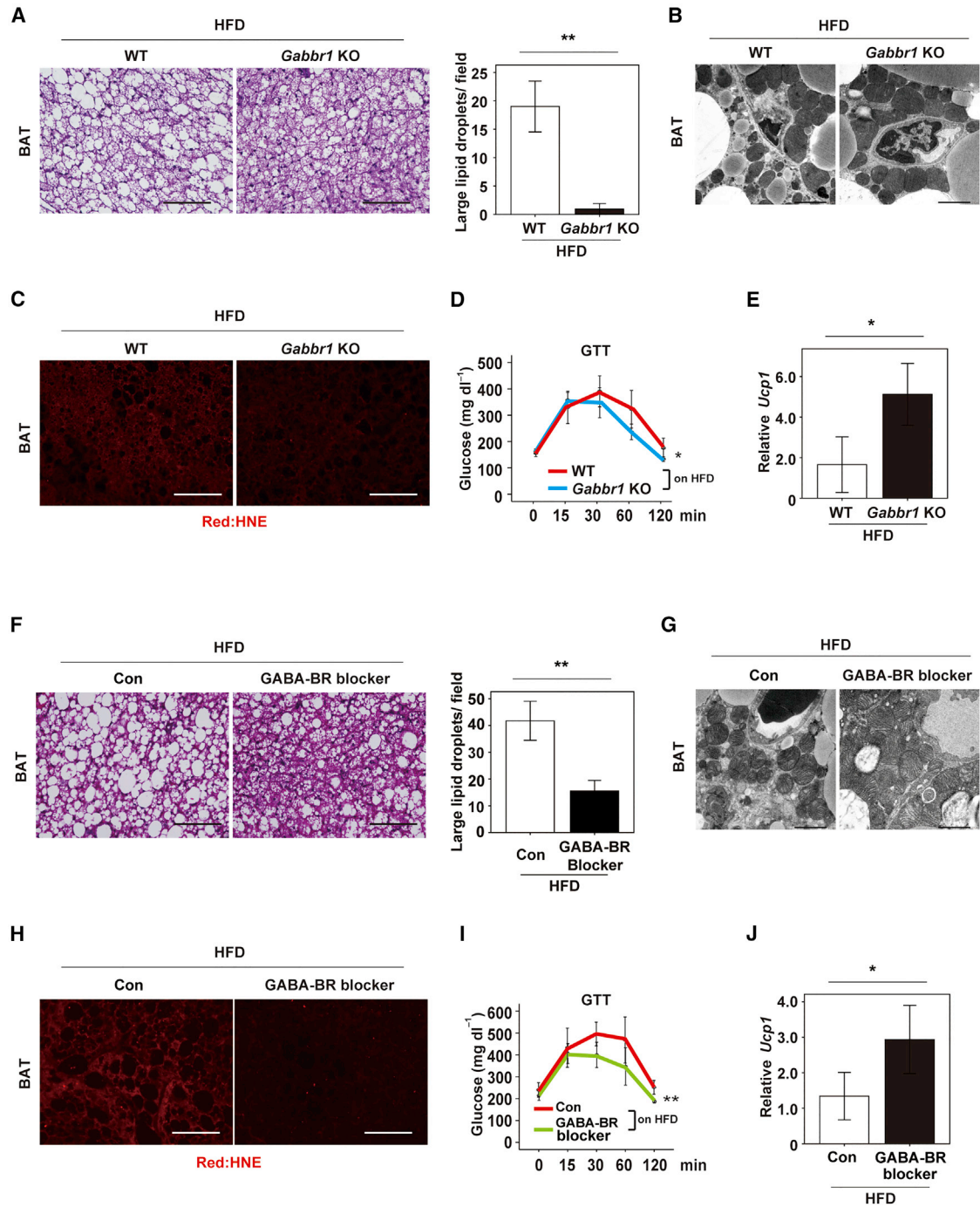


Figure 3. Inhibition of GABA-BR1-Mediated Signaling Suppresses Whitening of BAT and Improves Systemic Metabolic Health

Characterization of GABA-BR1 heterozygous knockout (*Gabbr1* KO) mice (18 weeks old) and mice with selective GABA-B receptor inhibition in BAT. Mice were fed the HFD from 4 weeks of age for a total of 14 weeks (*Gabbr1* KO mice) or 12 weeks (GABA-BR blocker mice). The mice were analyzed by H&E staining of interscapular BAT (A and F; scale bars = 100 μ m), transmission electron microscope study of BAT (B and G; scale bars = 2 μ m), and 4-HNE staining of BAT (C and H; scale bars = 100 μ m). Results of the glucose tolerance test (D [n = 6 and 9] and I [n = 4 and 4]). Results of qPCR for *Ucp1* in interscapular BAT (E [n = 5 and 5] and J [n = 8 and 5]). Right panels in (A) (n = 3 and 3) and (F) (n = 4 and 4) show quantitative data for the number of large lipid droplets (defined as >250 μ m²) per field. Data were analyzed by the two-tailed Student's t test (A, E, F, and J) or two-way ANOVA, followed by Tukey's multiple comparison test (D and I). *p < 0.05; **p < 0.01. Values represent the mean \pm SEM. Data are from one of two independent series of experiments (A and C), from one independent series of experiment (B and F–J), or from two independent series of experiments (D and E). All data are from different biological replicates.

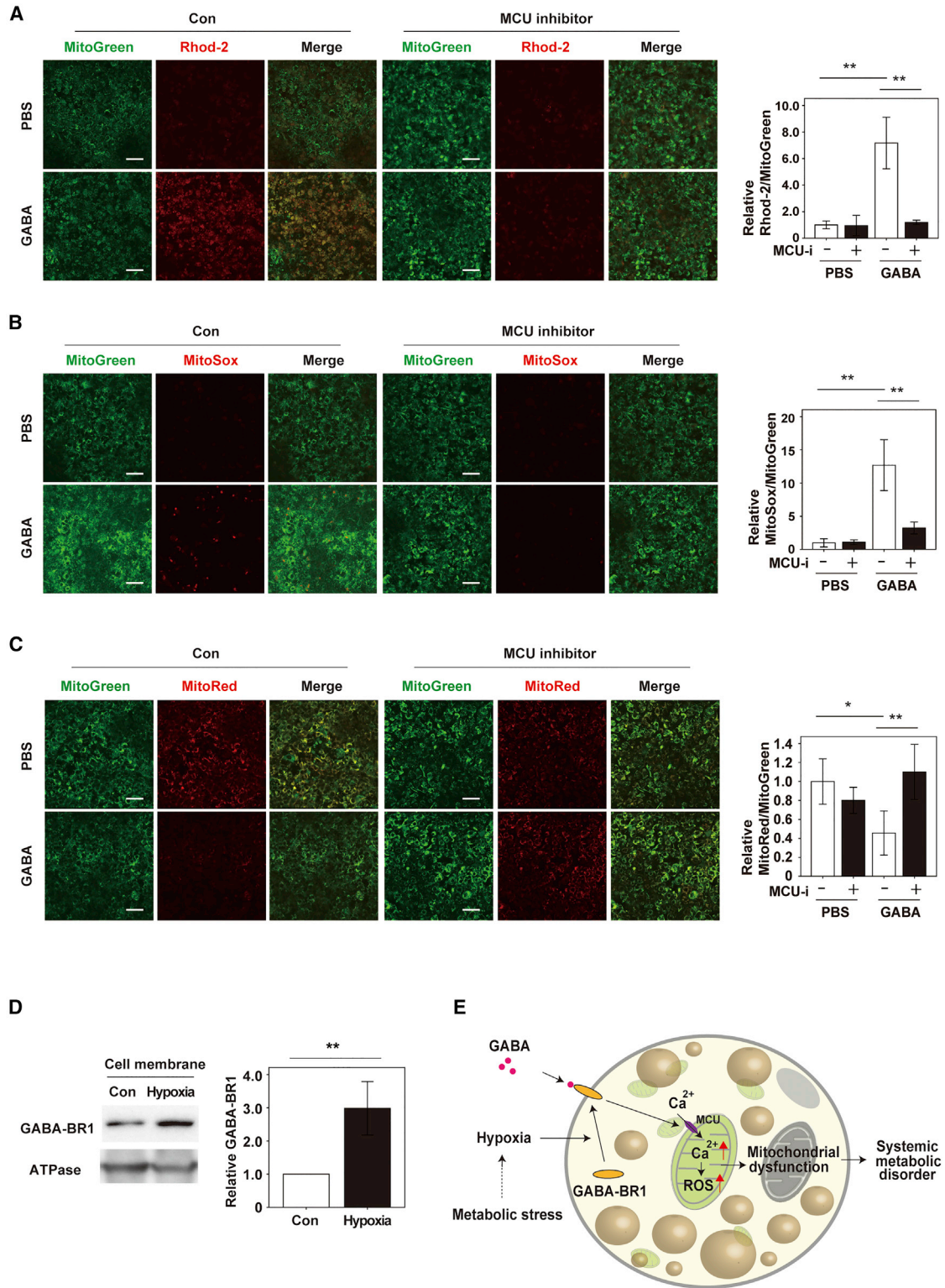


Figure 4. GABA/GABA-BR1-Mediated Signaling Induces Mitochondrial Calcium Overload and Dysfunction

(A–C) Relative staining of mitochondrial calcium (Rhod-2; A), mitochondrial reactive oxygen species (MitoSox; B), functional mitochondria (MitoRed; C), and total mitochondria (Mito Tracker Green FM [MitoGreen]) in differentiated brown adipocytes incubated with PBS or GABA (250 nM; 20 min for Rhod-2 and 250 nM; 6 hr for MitoRed or MitoGreen) with or without a calcium uniporter protein, mitochondrial inhibitor (MCU inhibitor; 250 nM; 20 min for Rhod-2 and 250 nM; 6 hr for

(legend continued on next page)

white adipose tissue (WAT), and skeletal muscle (quadriceps muscle) and found *Gabbr1* transcript levels remain unchanged in these organs following the injection of AAV sh-*Gabbr1* into the BAT (data not shown). Body weight and the BAT/body weight (BW) ratio were comparable between the AAV sh-*Gabbr1*-treated group and control groups (Figure S4C); however, BAT whitening was markedly improved by this treatment (Figure S4D). Electron microscopy showed that mitochondrial fragmentation and rarefaction in the brown adipocytes of interscapular BAT were also reduced in the AAV sh-*Gabbr1*-treated group compared to the control group (Figure S4E). ROS levels were also significantly reduced in the interscapular BAT of the AAV sh-*Gabbr1*-treated group (Figure S4F), and systemic glucose intolerance was improved in this group under dietary obese conditions (Figure S4G). These results indicate that a reduction in *Gabbr1* in BAT promotes the re-browning of BAT under conditions of metabolic stress, thereby contributing to systemic metabolic health.

GABA/GABA-BR1-Mediated Signaling Promotes Brown Adipocyte Dysfunction

We subsequently investigated the mechanisms that mediate brown adipocyte dysfunction downstream of GABA/GABA-BR1 signaling. The GABA-B receptor couples to G proteins, and its downstream signaling reportedly increases intracellular Ca^{2+} (Bazargani and Attwell, 2016; New et al., 2006). An increase of cytosolic Ca^{2+} promotes mitochondrial Ca^{2+} influx through calcium uniporter protein, mitochondrial (MCU) (Shanmughapriya et al., 2015; Wiel et al., 2014). In the mitochondria, calcium regulates enzymes of the citric acid cycle and helps to maintain mitochondrial homeostasis, and calcium overload increases mitochondrial ROS production and dysfunction (Arruda et al., 2014; Brookes et al., 2004; Görlach et al., 2015; Pinton et al., 2008). These findings led us to test whether GABA-BR1-mediated signaling causes an increase in the mitochondrial levels of Ca^{2+} and ROS. As expected, the addition of GABA to cultures of differentiated brown adipocytes increased both mitochondrial calcium and ROS (left panel in Figures 4A and 4B) and also reduced the mitochondrial membrane potential (left panel in Figure 4C); all of these changes were ameliorated by the administration of an MCU inhibitor (right panel in Figures 4A–4C). The results of Seahorse XF extracellular flux analysis for oxygen consumption rate indicated that GABA reduced mitochondrial respiration in differentiated brown adipocytes (Figure S4H). Similar to the effects of GABA, the addition of a selective calcium ionophore (ionomycin) to differentiated brown adipocyte cultures increased mitochondrial calcium and ROS levels and

reduced the mitochondrial membrane potential (Figures S4I–S4K). These findings suggest that the activation of GABA/GABA-BR1 signaling induces mitochondrial dysfunction in brown adipocytes by promoting excessive Ca^{2+} influx.

Finally, we studied the mechanisms by which metabolic stress contributes to the activation of GABA/GABA-BR1 signaling, focusing on the increase of GABA-BR1 immunoreactivity in the cell membranes of brown adipocytes in the BAT of obese mice. Obesity is reported to induce hypoxia in BAT by suppressing the production of vascular endothelial growth factor (Shimizu et al., 2014). Our *in vitro* studies showed that hypoxia promotes the translocation of GABA-BR1 to the cell membrane in brown adipocytes (Figure 4D), indicating that hypoxic stress might contribute to the activation of GABA-BR1-mediated signaling. In the CNS, GABA is reported to act after its uptake via the GABA transporter (Conti et al., 2004). To exclude the potential contribution of a GABA-GABA transporter pathway in brown adipocytes, we performed metabolic flux analysis with CE-MS. For this assay, primary brown adipocytes were prepared from the BAT of 2- to 3-day-old Wistar rats. The addition of stable isotope-labeled GABA (4-aminobutyric acid-2,2,3,3,4,4-d6 acid) to differentiated brown adipocytes showed that exogenous GABA did not pass through the cell membrane (Figure S4L), indicating that the pathways mediated by GABA-BR1, but not by the GABA transporter, are involved in the disturbance of brown adipocyte homeostasis.

DISCUSSION

The findings of our study suggest that the constitutive activation of GABA/GABA-BR1 signaling mediates BAT dysfunction and systemic metabolic derangement in conditions of obesity. Our findings show that GABA/GABA-BR1-mediated signaling triggered excessive calcium influx into the mitochondria of brown adipocytes in mice, via MCU, leading to mitochondrial calcium overload and to increased ROS production. Our findings also show that, in healthy volunteers, GABA-BR1 transcripts are significantly increased in individuals with low *UCP1* expression compared to those with high *UCP1* expression. Obesity is associated with the functional decline of BAT, and metabolic stress is reported to reduce *Ucp1* expression (Cypess et al., 2009; Shimizu et al., 2014). Our findings thus implicate GABA-BR1-mediated signaling in inducing BAT dysfunction in obese mice and demonstrate that *GABA-BR1* expression levels inversely correlate with *UCP1* expression in humans.

In this study, we could not completely characterize the mechanisms that lead to increased GABA in the BAT of our obese

MitoRed or MitoGreen). The scale bars represent 50 μm . Right panels in Figures 4A–4C show quantification of signals in the indicated groups (A: n = 4, 4, 4, and 4; B: n = 5, 5, 5, and 5; C: n = 4, 4, 4, and 4; MCU-i, MCU inhibitor).

(D) Western blot analysis of GABA-BR1 in the cell membranes of brown adipocytes under normoxic conditions (Con) or hypoxic conditions (1% O_2 for 1 hr; hypoxia). Right panel displays quantification of GABA-BR1 relative to the ATPase loading control (n = 3 and 3).

(E) Scheme showing a summary of the findings in this study. Under metabolic stress, BAT is reported to develop hypoxia (Shimizu et al., 2014), and our findings indicate that hypoxia promotes transition of GABA-BR1 to the cell membrane. GABA/GABA-BR1-mediated signaling induces calcium influx into mitochondria via calcium uniporter protein, mitochondrial (MCU), leading to calcium overload and increased production of reactive oxygen species (ROS). This results in mitochondrial dysfunction and systemic metabolic derangement.

Data were analyzed by the two-tailed Student's t test (D) with the non-parametric Kruskal-Wallis test (A) or by two-way ANOVA followed by Tukey's multiple comparison test (B and C). *p < 0.05; **p < 0.01. Values represent the mean \pm SEM. Data are from three independent series of experiment (A–C) or one of two independent series of experiments (D). All data are from different biological replicates.

mouse model. Our metabolomic analyses have suggested that circulating GABA levels would not be increased in our murine model of dietary obesity. Our findings show that the sympathetic denervation of BAT significantly reduced norepinephrine to an undetectable level but led to only a slight and non-significant reduction of GABA in the BAT of both the normal chow and HFD-fed groups. This suggests that the sympathetic nervous system might play only a minor role in regulating GABA levels in BAT during metabolic stress, as well as under physiological conditions. We also investigated whether brown adipocytes could generate GABA from glutamate by the GABA shunt. Our findings show this not to be the case: GAD1 and GAD2 proteins were not detected in the BAT of obese WT mice and *Gad1* and *Gad2* transcripts were not detected in either the BAT of obese WT mice or in differentiated brown adipocytes *in vitro*. However, low *Gad1* expression levels in CD45⁺ cells indicate that immune cells might make a minor contribution to GABA production in BAT under metabolic stress.

In differentiated brown adipocytes, our findings show that exogenous GABA did not cross the cell membrane (Figure S4L), but this does not necessarily exclude the existence of other GABA transporters involved in the excretion of intracellular GABA from brown adipocytes. GABA might have been increased in the BAT of the HFD group simply because membranous GABA-BR1 is upregulated by obesity, as shown in our study, but the existence of unknown metabolic pathways contributing to intracellular GABA production cannot be excluded and further studies are needed to explore the underlying mechanisms involved. In addition to its post-transcriptional regulation, we found that GABA-BR1 was transcriptionally upregulated in the chronic phase of dietary obesity. The levels of *Gabbr1* in the BAT of normal-chow-fed and HFD-fed mice after 10 weeks were comparable (data not shown), but *Gabbr1* was significantly increased in the HFD-fed mice after 20 weeks. In addition to the translocation of GABA-BR1 to the cell membrane in brown adipocytes, this result suggests that transcriptional activation contributes to the augmentation of GABA/GABA-BR1 signaling in the chronic phase of obesity.

Our findings also show that the suppression of excessive GABA/GABA-BR1 signaling and the inhibition of mitochondrial calcium overload in BAT is crucial for the maintenance of normal BAT function and contributes to healthy systemic metabolism (Figure 4E). Together, these findings advance our understanding of the pathological role that peripheral GABA signaling plays in BAT.

STAR★METHODS

Detailed methods are provided in the online version of this paper and include the following:

- KEY RESOURCES TABLE
- CONTACT FOR REAGENT AND RESOURCE SHARING
- EXPERIMENTAL MODEL AND SUBJECT DETAILS
 - Human samples
 - Animal models
- METHOD DETAILS
 - Systemic metabolic parameters
 - Acute cold exposure
 - Metabolomic analyses
 - Histological and physiological analyses
 - RNA analysis
 - Western blot analysis
 - Analysis of GAD expression
 - Brown adipocyte cell line and molecular probe studies
 - Extracellular Flux Assay
 - Adeno associated virus (AAV) and IVIS imaging system
- QUANTIFICATION AND STATISTICAL ANALYSIS

SUPPLEMENTAL INFORMATION

Supplemental Information includes four figures and can be found with this article online at <https://doi.org/10.1016/j.celrep.2018.08.024>.

ACKNOWLEDGMENTS

We thank Kaori Yoshida, Keiko Uchiyama, Satomi Kawai, Naomi Hatanaka, Ryoko Ito, Yoko Sawaguchi, Runa Washio, Masaaki Nameta (Niigata University), Kaori Igarashi, Kaori Saitoh, Keiko Endo, Hiroko Maki, Ayano Ueno, and Maki Ohishi (Keio University) for their excellent technical assistance and C. Ronald Kahn (Joslin Diabetes Center and Harvard Medical School) for providing the BAT cell line. This work was supported by a Grant-in-Aid for Scientific Research (grant number 17H04172), a Grant-in-Aid for Scientific Research on Innovative Areas (Stem Cell Aging and Disease; grant number 26115008), and a Grant-in-Aid for Exploratory Research from the Ministry of Education, Culture, Sports, Science and Technology (MEXT) (grant number 15K15306) of Japan and grants from the Takeda Medical Research Foundation, the Japan Foundation for Applied Enzymology, the Takeda Science Foundation, the SENSHIN Medical Research Foundation, the Terumo Foundation, the Manpei Suzuki Diabetes Foundation, the Naito Foundation, and the Novartis Foundation (to T.M.); as well as by a Grant-in-Aid for Young Scientists (Start-up; Japan Society for the Promotion of Science [JSPS] KAKENHI; grant number 26893080) and grants from the Uehara Memorial Foundation, Kowa Life Science Foundation, Ono Medical Research Foundation, The Nakajima Foundation, Suzuken Memorial Foundation, Grants-in-Aid for Encouragement of Young Scientists (A) (JSPS KAKENHI grant number 16H06244), Grant-in-Aid for Challenging Exploratory Research (JSPS KAKENHI grant number 17K19648), Japan Agency for Medical Research and Development (AMED) under grant number JP17gm5010002, and Astellas Foundation for Research on Metabolic Disorders (to I.S.); by a Grant-in-Aid for Encouragement of Young Scientists (B) (JSPS KAKENHI grant number 16K19531; to Y.Y.); and by a grant from Bourbon (to T.M., I.S., and Y.Y.). The Centre for Physical Activity Research (CFAS) is supported by a grant from TrygFonden. During the study period, the Centre of Inflammation and Metabolism (CIM) was supported by a grant from the Danish National Research Foundation (DNRF55).

AUTHOR CONTRIBUTIONS

T.M. and I.S. designed the study and wrote the manuscript. R.I., I.S., and T. Sato performed most of the experiments. Y.H., M.S., G.K., J.L., and T.W. performed the *in vitro* study. Y.Y. and E.H. performed the *in vivo* study. Y.M. and S.O. provided technical help. S.N., N.Z.J., and C.S. collected and analyzed human samples.

DECLARATION OF INTERESTS

The authors declare no competing interests.

Received: May 5, 2017

Revised: May 30, 2018

Accepted: August 8, 2018

Published: September 11, 2018

REFERENCES

- Adeghate, E., and Ponery, A.S. (2002). GABA in the endocrine pancreas: cellular localization and function in normal and diabetic rats. *Tissue Cell* *34*, 1–6.
- Al-Salam, S., Hameed, R., Parvez, H.S., and Adeghate, E. (2009). Diabetes mellitus decreases the expression of calcitonin-gene related peptide, gamma-amino butyric acid and glutamic acid decarboxylase in human pancreatic islet cells. *Neuroendocrinol. Lett.* *30*, 506–510.
- Aruda, A.P., Pers, B.M., Parlakgöl, G., Güney, E., Inouye, K., and Hotamisligil, G.S. (2014). Chronic enrichment of hepatic endoplasmic reticulum-mitochondria contact leads to mitochondrial dysfunction in obesity. *Nat. Med.* *20*, 1427–1435.
- Bartelt, A., Bruns, O.T., Reimer, R., Hohenberg, H., Ittrich, H., Peldschus, K., Kaul, M.G., Tromsdorf, U.I., Weller, H., Waurisch, C., et al. (2011). Brown adipose tissue activity controls triglyceride clearance. *Nat. Med.* *17*, 200–205.
- Bazargani, N., and Attwell, D. (2016). Astrocyte calcium signaling: the third wave. *Nat. Neurosci.* *19*, 182–189.
- Boonstra, E., de Kleijn, R., Colzato, L.S., Alkemade, A., Forstmann, B.U., and Nieuwenhuis, S. (2015). Neurotransmitters as food supplements: the effects of GABA on brain and behavior. *Front. Psychol.* *6*, 1520.
- Brookes, P.S., Yoon, Y., Robotham, J.L., Anders, M.W., and Sheu, S.S. (2004). Calcium, ATP, and ROS: a mitochondrial love-hate triangle. *Am. J. Physiol. Cell Physiol.* *287*, C817–C833.
- NCD Risk Factor Collaboration (NCD-RisC) (2017). Worldwide trends in body-mass index, underweight, overweight, and obesity from 1975 to 2016: a pooled analysis of 2416 population-based measurement studies in 128.9 million children, adolescents, and adults. *Lancet* *390*, 2627–2642.
- Conti, F., Minelli, A., and Melone, M. (2004). GABA transporters in the mammalian cerebral cortex: localization, development and pathological implications. *Brain Res. Brain Res. Rev.* *45*, 196–212.
- Crane, J.D., Palanivel, R., Mottillo, E.P., Bujak, A.L., Wang, H., Ford, R.J., Collins, A., Blümer, R.M., Fullerton, M.D., Yabut, J.M., et al. (2015). Inhibiting peripheral serotonin synthesis reduces obesity and metabolic dysfunction by promoting brown adipose tissue thermogenesis. *Nat. Med.* *21*, 166–172.
- Cypess, A.M., Lehman, S., Williams, G., Tal, I., Rodman, D., Goldfine, A.B., Kuo, F.C., Palmer, E.L., Tseng, Y.H., Doria, A., et al. (2009). Identification and importance of brown adipose tissue in adult humans. *N. Engl. J. Med.* *360*, 1509–1517.
- Dawkins, M.J., and Scopes, J.W. (1965). Non-shivering thermogenesis and brown adipose tissue in the human new-born infant. *Nature* *206*, 201–202.
- Fasshauer, M., Klein, J., Kriauciunas, K.M., Ueki, K., Benito, M., and Kahn, C.R. (2001). Essential role of insulin receptor substrate 1 in differentiation of brown adipocytes. *Mol. Cell. Biol.* *21*, 319–329.
- Fukui, M., Nakamichi, N., Yoneyama, M., Ozawa, S., Fujimori, S., Takahata, Y., Nakamura, N., Taniura, H., and Yoneda, Y. (2008). Modulation of cellular proliferation and differentiation through GABA(B) receptors expressed by undifferentiated neural progenitor cells isolated from fetal mouse brain. *J. Cell. Physiol.* *216*, 507–519.
- Gladkevich, A., Korf, J., Hakobyan, V.P., and Melkonyan, K.V. (2006). The peripheral GABAergic system as a target in endocrine disorders. *Auton. Neurosci.* *124*, 1–8.
- Görlach, A., Bertram, K., Hudecova, S., and Krizanova, O. (2015). Calcium and ROS: A mutual interplay. *Redox Biol.* *6*, 260–271.
- Harms, M., and Seale, P. (2013). Brown and beige fat: development, function and therapeutic potential. *Nat. Med.* *19*, 1252–1263.
- Hirayama, A., Kami, K., Sugimoto, M., Sugawara, M., Toki, N., Onozuka, H., Kinoshita, T., Saito, N., Ochiai, A., Tomita, M., et al. (2009). Quantitative metabolome profiling of colon and stomach cancer microenvironment by capillary electrophoresis time-of-flight mass spectrometry. *Cancer Res.* *69*, 4918–4925.
- Jespersen, N.Z., Larsen, T.J., Pejts, L., Daugaard, S., Homøe, P., Loft, A., de Jong, J., Mathur, N., Cannon, B., Nedergaard, J., et al. (2013). A classical brown adipose tissue mRNA signature partly overlaps with brite in the supraclavicular region of adult humans. *Cell Metab.* *17*, 798–805.
- Klein, J., Fasshauer, M., Ito, M., Lowell, B.B., Benito, M., and Kahn, C.R. (1999). beta(3)-adrenergic stimulation differentially inhibits insulin signaling and decreases insulin-induced glucose uptake in brown adipocytes. *J. Biol. Chem.* *274*, 34795–34802.
- Ko, J., Choi, G., and Um, J.W. (2015). The balancing act of GABAergic synapse organizers. *Trends Mol. Med.* *21*, 256–268.
- Li, C., Liu, C., Nissim, I., Chen, J., Chen, P., Doliba, N., Zhang, T., Nissim, I., Daikhin, Y., Stokes, D., et al. (2013). Regulation of glucagon secretion in normal and diabetic human islets by γ -hydroxybutyrate and glycine. *J. Biol. Chem.* *288*, 3938–3951.
- Li, J., Casteels, T., Frogne, T., Ingvorsen, C., Honoré, C., Courtney, M., Huber, K.V.M., Schmitner, N., Kimmel, R.A., Romanov, R.A., et al. (2017). Artemisinins target GABAA receptor signaling and impair α cell identity. *Cell* *168*, 86–100.e15.
- Nedergaard, J., Golozoubova, V., Matthias, A., Asadi, A., Jacobsson, A., and Cannon, B. (2001). UCP1: the only protein able to mediate adaptive non-shivering thermogenesis and metabolic inefficiency. *Biochim. Biophys. Acta* *1504*, 82–106.
- New, D.C., An, H., Ip, N.Y., and Wong, Y.H. (2006). GABAB heterodimeric receptors promote Ca²⁺ influx via store-operated channels in rat cortical neurons and transfected Chinese hamster ovary cells. *Neuroscience* *137*, 1347–1358.
- Patel, A.B., de Graaf, R.A., Mason, G.F., Rothman, D.L., Shulman, R.G., and Behar, K.L. (2005). The contribution of GABA to glutamate/glutamine cycling and energy metabolism in the rat cortex in vivo. *Proc. Natl. Acad. Sci. USA* *102*, 5588–5593.
- Pinton, P., Giorgi, C., Siviero, R., Zecchini, E., and Rizzuto, R. (2008). Calcium and apoptosis: ER-mitochondria Ca²⁺ transfer in the control of apoptosis. *Oncogene* *27*, 6407–6418.
- Prentki, M., Matschinsky, F.M., and Madiraju, S.R.M. (2013). Metabolic signaling in fuel-induced insulin secretion. *Cell Metab.* *18*, 162–185.
- Schuler, V., Lüscher, C., Blanchet, C., Klix, N., Sansig, G., Klebs, K., Schmutz, M., Heid, J., Gentry, C., Urban, L., et al. (2001). Epilepsy, hyperalgesia, impaired memory, and loss of pre- and postsynaptic GABA(B) responses in mice lacking GABA(B1). *Neuron* *31*, 47–58.
- Sen, S., Roy, S., Bandyopadhyay, G., Scott, B., Xiao, D., Ramadoss, S., Mahata, S.K., and Chaudhuri, G. (2016). γ -aminobutyric acid is synthesized and released by the endothelium: potential implications. *Circ. Res.* *119*, 621–634.
- Shanmughapriya, S., Rajan, S., Hoffman, N.E., Zhang, X., Guo, S., Kolesar, J.E., Hines, K.J., Ragheb, J., Jog, N.R., Caricchio, R., et al. (2015). Ca²⁺ signals regulate mitochondrial metabolism by stimulating CREB-mediated expression of the mitochondrial Ca²⁺ uniporter gene MCU. *Sci. Signal.* *8*, ra23.
- Shimizu, I., and Walsh, K. (2015). The whitening of brown fat and its implications for weight management in obesity. *Curr. Obes. Rep.* *4*, 224–229.
- Shimizu, I., Aprahamian, T., Kikuchi, R., Shimizu, A., Papanicolaou, K.N., MacLauchlan, S., Maruyama, S., and Walsh, K. (2014). Vascular rarefaction mediates whitening of brown fat in obesity. *J. Clin. Invest.* *124*, 2099–2112.
- Shinoda, K., Luijten, I.H., Hasegawa, Y., Hong, H., Sonne, S.B., Kim, M., Xue, R., Chondronikola, M., Cypess, A.M., Tseng, Y.H., et al. (2015). Genetic and functional characterization of clonally derived adult human brown adipocytes. *Nat. Med.* *21*, 389–394.
- Smith, R.E., and Roberts, J.C. (1964). Thermogenesis of brown adipose tissue in cold-acclimated rats. *Am. J. Physiol.* *206*, 143–148.
- Stanford, K.I., Middelbeek, R.J., Townsend, K.L., An, D., Nygaard, E.B., Hitchcox, K.M., Markan, K.R., Nakano, K., Hirshman, M.F., Tseng, Y.H., and Goodyear, L.J. (2013). Brown adipose tissue regulates glucose homeostasis and insulin sensitivity. *J. Clin. Invest.* *123*, 215–223.
- Tang, L., Okamoto, S., Shiuchi, T., Toda, C., Takagi, K., Sato, T., Saito, K., Yokota, S., and Minokoshi, Y. (2015). Sympathetic nerve activity maintains

an anti-inflammatory state in adipose tissue in male mice by inhibiting TNF- α gene expression in macrophages. *Endocrinology* 156, 3680–3694.

Tong, Q., Ye, C.P., Jones, J.E., Elmquist, J.K., and Lowell, B.B. (2008). Synaptic release of GABA by AgRP neurons is required for normal regulation of energy balance. *Nat. Neurosci.* 11, 998–1000.

Turenius, C.I., Htut, M.M., Prodon, D.A., Ebersole, P.L., Ngo, P.T., Lara, R.N., Wilczynski, J.L., and Stanley, B.G. (2009). GABA(A) receptors in the lateral hypothalamus as mediators of satiety and body weight regulation. *Brain Res.* 1262, 16–24.

Wiel, C., Lallet-Daher, H., Gitenay, D., Gras, B., Le Calvé, B., Augert, A., Ferrand, M., Prevarskaya, N., Simonnet, H., Vindrieux, D., et al. (2014). Endoplasmic reticulum calcium release through ITPR2 channels leads to mitochondrial calcium accumulation and senescence. *Nat. Commun.* 5, 3792.

Xu, Y., O'Brien, W.G., 3rd, Lee, C.C., Myers, M.G., Jr., and Tong, Q. (2012). Role of GABA release from leptin receptor-expressing neurons in body weight regulation. *Endocrinology* 153, 2223–2233.

Yoshida, Y., Shimizu, I., Katsuami, G., Jiao, S., Suda, M., Hayashi, Y., and Minamino, T. (2015). p53-Induced inflammation exacerbates cardiac dysfunction during pressure overload. *J. Mol. Cell. Cardiol.* 85, 183–198.

STAR★METHODS

KEY RESOURCES TABLE

REAGENT or RESOURCE	SOURCE	IDENTIFIER
Antibodies		
Anti-GABA antibody	Sigma Aldrich	A2052; RRID: AB_477652
GABA-BR1 antibody	Santa Cruz	sc-7338; RRID: AB_640742
Anti-GABA-BR1 antibody	Abcam	ab166604; RRID: N/A
Anti-actin antibody	Cell Signaling	#4967; RRID: AB_330288
Anti-UCP1	Abcam	ab10983; RRID: AB_2241462
Anti- α -tubulin	Cell Signaling	#2125; RRID: AB_2619646
Anti-sodium potassium ATPase antibody	Abcam	ab76020; RRID: AB_1310695
Anti-4 hydroxynoneal antibody	Abcam	ab46545; RRID: AB_722390
Hoechst	Life Technologies	33258; RRID: AB_2651133
Goat anti-rabbit IgG H&L (Cy5)	Abcam	ab97077; RRID: AB_10679461
Goat anti-rabbit IgG H&L (DyLight488)	Abcam	ab96899; RRID: AB_10679361
Donkey anti-goat IgG H&L (Cy5)	Abcam	ab6566; RRID: AB_955056
Horseradish peroxidase-conjugated anti-rabbit immunoglobulin G	Jackson ImmunoResearch	#113-035-003; RRID: AB_2313567
Anti-GAD65+GAD67 antibody	Abcam	ab183999; RRID: N/A
Rat anti-mouse CD45	BD Biosciences	550539; RRID: AB_2174426
Dynabeads sheep anti-rat IgG	Invitrogen	11035; RRID: N/A
Bacterial and Virus Strains		
AAV-DJ Helper Free shRNA Expression System	Cell Biolabs Inc	VPK-413-DJ
Biological Samples		
BAT cDNA samples from Human	Dr. Camilla Scheele	Rigshospitalet, Copenhagen, Denmark
Chemicals, Peptides, and Recombinant Proteins		
GABA-B receptor antagonist, SCH-50911	TOCRIS Bioscience	0984
GABA	Sigma Aldrich	A5835
Ionomycin	WAKO	095-05831
MCU inhibitor, KB-R7943	TOCRIS Bioscience	1244
Wheat germ agglutinin, Alexa Fluor 488 conjugate	Thermo Fisher Scientific	W11261
Dihydroethidium (DHE)	WAKO	041-28251
MitoSox	Thermo Fisher Scientific	M36008
MitoTracker Green FM	Thermo Fisher Scientific	M7514
MitoTracker Red CM-H2Xros	Thermo Fisher Scientific	M7513
Rhod-2 AM	Thermo Fisher Scientific	R1245MP
Critical Commercial Assays		
Plasma membrane protein extraction kit	Abcam	ab65400
QuickTiter AAV Quantitation Kit	Cell Biolabs Inc	VPK-145
ViraBind AAV Purification Kit	Cell Biolabs Inc	VPK-140
X-tremeGENE9 DNA Transfection Reagent	Roche	06365809001
Experimental Models: Cell Lines		
Brown pre-adipocytes	Dr. C. Ronald Kahn	(Klein et al., 1999)
Oligonucleotides		
Sequence of sh-Gabbr1	In this paper	N/A
5'-GATCCGCGGTTTCCAACGTTCTTTTCTCGAAGAGACGAAAGAAC GTTGGAAACCGCTTTTTTG-3'		

(Continued on next page)

Continued

REAGENT or RESOURCE	SOURCE	IDENTIFIER
Sequence of sh-Gabbr1 complement	In this paper	N/A
5'-AATTCAAAAAAGCGGTTTCCAACGTTCTTTTCGTCTCTTCGAA AGAACGTTGGAAACCGCG-3'		

CONTACT FOR REAGENT AND RESOURCE SHARING

Further information and requests for resources and reagents should be directed to and will be fulfilled by the Lead Contact, Tohru Minamino (tminamino@med.niigata-u.ac.jp, t_minamino@yahoo.co.jp).

EXPERIMENTAL MODEL AND SUBJECT DETAILS**Human samples**

Supraclavicular adipose tissue samples from a previous study were used (Jespersen et al., 2013). Briefly, prior to elective surgery, patients with suspected head and neck cancer were enrolled via the outpatient clinic of the Department of Oto-Rhino-Laryngology Head & Neck Surgery at Rigshospitalet (Copenhagen, Denmark). All subjects provided written informed consent prior to participation. The Scientific-Ethics Committees of the Capital Region and of Copenhagen and Frederiksberg Municipalities, Denmark approved the study protocols (journal number H-A-2009-020 and H-17014258 respectively), and the studies were performed in accordance with the Declaration of Helsinki. Biopsies were obtained during surgery by an experienced surgeon. Tissue was removed using a scalpel and scissors. Immediately after removal, the tissue samples were flash frozen in liquid nitrogen before being stored at -80°C until analysis. Due to variation of UCP1 expression, supraclavicular samples were divided into high BAT (Mean BMI = 24, Median BMI = 24, ranging from BMI 20-28) and low BAT groups (Mean BMI = 25, Median BMI = 26, ranging from BMI 18-31) based on UCP1 expression ($n = 10$ (female ($n = 6$) and male ($n = 4$)) and $n = 9$ (female ($n = 3$), male ($n = 6$)) respectively), as described previously (Jespersen et al., 2013). qPCR studies were performed using the ViiA 7 Real-Time PCR System (Thermo Fisher Scientific). PPIA gene expression was determined by using Power Up SYBR Green Master Mixgreen with standard settings. GABA-BR1 gene expression was assessed with TaqMan Universal PCR Master Mix. Results were normalized for PPIA and calculated by the standard curve method. Assays were conducted using UCP1 (Hs00222453_m1) or GABBR1: (Hs00961677_m1).

The other primers and their sequences were as follows.

GABBR1; 5'-Cccgacttccatctggtg-3', 5'-gtggcgttcgattcacct-3'
PPIA; 5'-acgccaccgcccaggaaaac-3', 5'-tgcaaacagctcaaggagacgc-3'

Animal models

All of the animal experiments were conducted in compliance with the protocol reviewed by the Institutional Animal Care and Use Committee of Niigata University and approved by the President of Niigata University. C57BL/6Ncr male mice were purchased from SLC Japan (Shizuoka, Japan). These mice were maintained on a high fat diet (HFD)(HFD32, CLEA Japan) for 9–16 weeks, starting at 4 weeks of age, unless otherwise described in the figure legends. In some normal chow (NC) and HFD groups, gamma-aminobutyric acid (GABA) (Sigma Aldrich, A5835) was added to the drinking water at 2 mg/ml from 4 weeks of age. In some HFD groups, a selective GABA-B receptor antagonist (SCH-50911; TOCRIS Bioscience, 0984; total dose: 450 $\mu\text{g}/\text{mouse}$) was administered around the interscapular BAT via an infusion pump with vinyl catheter tubing (Durect Corp.) for 2 weeks from 14 weeks of age, and the mice were subjected to analysis at 16 weeks. GABA-BR1 heterozygous knockout (*Gabbr1* KO) male mice were generated on a BALB/c background and were provided by Eiichi Hinoi (Kanazawa University, Ishikawa, Japan). Genotyping of these mice was conducted as described previously (Fukui et al., 2008). Heterozygous male mice were fed a high fat diet for at least 10 weeks from 4 weeks of age before undergoing investigation. Unilateral surgical denervation of interscapular BAT was performed as described previously (Tang et al., 2015).

METHOD DETAILS**Systemic metabolic parameters**

Mice were housed individually for one week prior to the assay. On the day of the glucose tolerance test, the mice were fasted for 6 hr and then glucose was injected intraperitoneally at a dose of 2g/kg in the early afternoon. Blood glucose levels were measured with a glucose analyzer (SANWA KAGAKU KENKYUSHO) at 15, 30, 60, and 120 min after glucose injection.

Acute cold exposure

Body temperature was assessed by subcutaneous implantation of biocompatible and sterile microchip transponders (IPTT-300 Extended Accuracy Calibration; Bio Medic Data Systems) in the scapular region according to the manufacturer's instructions. Animals were subjected to the cold tolerance test (CTT) at 4°C and body temperature was measured at hourly intervals for 6–8 hr.

Metabolomic analyses

Metabolomic analyses were done by Soga et al. using capillary electrophoresis-mass spectrometry (CE-MS), as described previously (Hirayama et al., 2009). Interscapular BAT samples from C57BL/6Ncr male mice were corrected and subjected to metabolomic studies to analyze the level of neurotransmitters. Flux analysis was performed *in vitro* with deuterated GABA (4-aminobutyric acid-2,2,3,3,4,4-d6 acid, Taiyo Nippon Sanso, 61558-7). For this assay, primary brown adipocytes were prepared from the BAT of 2- to 3-day-old Wistar rats. In brief, interscapular BAT was removed and washed in ice-cold PBS, after which it was minced finely and washed again with cold PBS. Isolation of cells was performed at 37°C by using collagenase (final concentration 12.5mg/ml), 0.9% NaCl (final concentration 0.123M), KCl (final concentration 5mM), CaCl₂ (final concentration 1.3 mM), glucose (final concentration 5mM), HEPES (final concentration 100 mM), and bovine serum albumin (final concentration 4%). After each digestion, the cell suspension was immediately placed in high glucose DMEM with 10% FBS and 100U/ml Penicillin/Streptomycin (P/S). After all digestions, the cell suspension was centrifuged for 5 minutes at 1,500 rpm in high glucose DMEM. Then the pellet was re-suspended in culture medium (high glucose DMEM with 10% FBS and 100 U/ml P/S). For use in further studies, cells were maintained at 37 °C with a 5% CO₂ atmosphere and differentiation was induced as previously described (Fasshauer et al., 2001). Fully differentiated brown adipocytes were used for analysis after 10 days of differentiation culture. After 12 nM 4-aminobutyric acid-2,2,3,3,4,4,d6 acid was added to the culture medium, cells were harvested at the indicated time points. Cells were washed three times with ice cold 5% Mannitol and then let stand for 10 min at room temperature in methanol containing L-methionine sulfone (25 μM, Wako 502-76641), MES (25 μM, Dojindo 349-01623), and CSA (25 μM, Wako 037-01032). The cells were harvested with a cell scraper and 400 μL of supernatant was collected after vortexing for 30 s. After adding CHCl₃ (400 μl) and distilled water (200 μl) with thorough mixing, centrifugation was performed at 10,000 g for 3 min at 4°C. Then the aqueous layer (400 μl) was transferred to an ultrafiltration tube (UltrafreeMC-PLHCC, Human Metabolome Technologies, UFC3LCCNB-HMT). This was followed by centrifugation at 9,100 g for 2hr at 20°C. Then 320 μL of filtrate was shipped to the Institute for Advanced Biosciences at Keio University for further analyses. In one study (Figure S3D), the norepinephrine level was measured in BAT with an ELISA kit (Abnova, Norepinephrine ELISA kit, KA1891).

Histological and physiological analyses

Interscapular BAT samples were harvested from mice, fixed overnight in 10% formalin, embedded in paraffin, and sectioned for immunofluorescence or hematoxylin-eosin (HE) staining. Lipid droplets and fluorescence signals were quantified with Image-J software at a magnification of x400, with four fields being randomly selected in each section. Large lipid droplets were defined as > 250 μm² in size. The following antibodies were used: anti-GABA antibody (Sigma Aldrich A2052), GABA-BR1 antibody (Santa Cruz Biotechnology sc-7338), anti-4 hydroxynoneal antibody (Abcam, ab46545), wheat germ agglutinin, Alexa Fluor 488 conjugate for staining cell membranes (Thermo Fisher Scientific, W11261), and Hoechst (Life Technologies, 33258). The secondary antibody for anti-GABA antibody was goat anti-rabbit IgG H&L (Cy5) (Abcam, ab97077) or goat anti-rabbit IgG H&L (DyLight488) (Abcam, ab96899). The secondary antibody for GABA-BR1 antibody was donkey anti-goat IgG H&L (Cy5) (Abcam, ab6566), while that for anti-4 hydroxynoneal antibody was goat anti-rabbit IgG H&L (Cy5) (Abcam, ab97077). In some studies, reactive oxygen species (ROS) was evaluated with Dihydroethidium (DHE) staining (WAKO, 041-28251). All primary and secondary antibodies were used at a dilution of 1:50, except for Hoechst (1:1000). Stained sections were photographed with a Biorevo (Keyence Co.). For electron microscopy, interscapular BAT was fixed in 2.5% glutaraldehyde/2.0% paraformaldehyde in 0.1M cacodylate buffer. Then 50 mg of calcium chloride was added to 400 mL of fixative. Grids for electron microscopy were prepared by Masaaki Nameta at the electron microscope core facility of Niigata University, and electron microscopy was performed by using a JEM1400 TEM at Niigata University Medical Campus.

RNA analysis

Total RNA (1 μg) was isolated from tissue samples with RNA-Bee (TEL-TEST Inc.). Real-time PCR (qPCR) was performed by using a Light Cycler 480 (Roche) with the Universal Probe Library and the Light Cycler 480 Probes Master (Roche) according to the manufacturer's instructions. The primers and their sequences were as follows. *Actb*, *Rps1*, or *Rplp0* was used as the internal control.

Actb; 5'-CTAAGGCCAACCGTAAAAG-3', 5'-ACCAGAGGCATACAGGGACA-3'
Rps18; 5'-GCTCTAGAATTACCACAGTTATCCAA-3', 5'-AAATCAGTTATGGTTCCTTTGGTC-3'
Gabbr1; 5'-CAACGTCACCTCGGAAGG-3', 5'-CGGCACACATATTCAATCTCA-3'
Ucp1; 5'-GGCCTCTACGACTCAGTCCA-3', 5'-TAAGCCGGCTGAGATCTTGT-3'
Mtn5; 5'-GGAAGCATCTTTGCAGGATT-3', 5'-TGGTATTGTGAGGATTGGAATG-3'
Ndufa1; 5'-TGATGGAACGCATAGACG-3', 5'-GCCAGGAAAATGCTTCCTTA-3'
Ppargc1a; 5'-GAAAGGGCCAAACAGAGAGA-3', 5'-GTAAATCACACGGCGCTCTT-3'
Rplp0 5'- gatgccagggaagacag -3', 5'- acaatgaagcattttggataa -3'

Western blot analysis

Whole-cell lysates were prepared in lysis buffer (10 mM Tris-HCl, pH 8, 140 mM NaCl, 5 mM EDTA, 0.025% NaN₃, 1% Triton X-100, 1% deoxycholate, 0.1% SDS, 1 mM PMSF, 5 μg ml⁻¹ leupeptin, 2 μg ml⁻¹ aprotinin, 50 mM NaF, and 1 mM Na₂VO₃). Then the lysates (40–50 μg) were resolved by SDS-PAGE. Proteins were transferred to a PVDF membrane (Millipore) that was incubated with the primary antibody, followed by incubation with horseradish peroxidase-conjugated anti-rabbit immunoglobulin G (Jackson

Immunoresearch, #113-035-003). Proteins were detected by enhanced chemiluminescence (GE). For western blotting of the plasma membrane fraction, we used a plasma membrane protein extraction kit (Abcam, ab65400). The primary antibodies for western blotting were anti-GABA-BR1 antibody (Abcam, ab166604), anti-actin antibody (Cell Signaling, #4967), anti-UCP1 (Abcam, ab10983), anti- α -tubulin (Cell Signaling, #2125), and anti-sodium potassium ATPase antibody (Abcam, ab76020). The primary antibodies were used at a dilution of 1:5000 for anti-GABA-BR1 antibody, 1:1000 for anti- α -tubulin, 1:2000 for anti-UCP1, and anti-actin antibody or 1:15000 for anti-sodium potassium ATPase antibody.

Analysis of GAD expression

Whole cell lysates were extracted from the BAT of mice fed NC or an HFD and subjected to western blot analysis as described above. The primary antibodies were anti-GAD65+GAD67 antibody (Abcam, ab183999) and anti- β -actin antibody (Cell Signaling, #4970) at a 1:1000 dilution. Total RNA was isolated from the BAT of mice fed NC or an HFD, as well as from mouse brain tissue and a brown adipocyte cell line, by using RNA-Bee (TEL-TEST Inc.). Magnetic-activated cell sorting was performed to harvest CD45⁺ cells from the BAT of mice fed an HFD by using rat anti-mouse CD45 (20:1 dilution, BD Biosciences, 550539) pre-conjugated with Dynabeads sheep anti-rat IgG (200 μ l, Invitrogen, 11035) and incubation overnight at 4°C, as reported previously (Yoshida et al., 2015). Then total RNA was isolated from the collected CD45⁺ cells and subjected to qPCR as described above with the following primers:

Gad1 (5'-ATACAACCTTTGGCTGCATGT -3', 5'-TTCCGGGACATGAGCAGT -3') and
Gad2 (5'-TGTAGCTGACATCTGCAAAAAGTA-3', 5'-GGGACATCAGTAACCCCTCCA-3').

Brown adipocyte cell line and molecular probe studies

The brown pre-adipocyte cell line was a kind gift from Dr. C. Ronald Kahn (Joslin Diabetes Center and Harvard Medical School, Section on Integrative Physiology and Metabolism, Boston, USA) (Klein et al., 1999). The cell line was established from wild-type FVB mice, and was immortalized by infection with the retroviral vector pBabe encoding SV40T antigen. Cells were cultured in high glucose DMEM with 10% FBS and 100 U/ml P/S, and differentiation was induced as described previously (Fasshauer et al., 2001). Fully differentiated brown adipocytes were used for further analysis after 10 days of culture. The brown adipocytes were stained with mitochondrial molecular probes and analyzed under an FV1200 confocal microscope (Olympus). MitoSox (1 μ M, 10 min, Thermo Fisher Scientific, M36008), MitoTracker Green FM (200 nM, 45 min, Thermo Fisher Scientific, M7514), MitoTracker Red CM-H2Xros (200 nM, 45 min, Thermo Fisher Scientific, M7513), and Rhod-2 AM (5 μ M, 30 min, Thermo Fisher Scientific, R1245MP) were used according to the instructions of the manufacturers. In some studies, differentiated brown adipocytes were cultured with GABA (250 nM for 6 hours; Sigma Aldrich, A5835), a GABA-B receptor antagonist (SCH 50911) (10 μ M, added 30 min before addition of GABA; TOCRIS Bioscience, 0984), ionomycin (10 μ M for 30 min (diluted with methanol); WAKO 095-05831), or an MCU inhibitor (KB-R7943) (250 nM, added simultaneously with GABA; TOCRIS Bioscience, 1244). Hypoxic stress was induced by culturing cells under hypoxic conditions (1% O₂ for 1 hr) in a hypoxia chamber (Stem Cell Technologies) according to the manufacturer's instructions.

Extracellular Flux Assay

The cellular oxygen consumption rate and extracellular acidification rate were measured with a Seahorse XF extracellular flux analyzer according to the manufacturer's instructions (Agilent Technologies). Brown pre-adipocytes were seeded in a Seahorse XF 24-well assay plate in high glucose DMEM with 10% FBS and 100 U/ml P/S at a density of 2,000 cells per well, and differentiation was initiated after 12 hr. After 4 days of differentiation culture, the differentiated adipocytes were incubated with PBS or GABA (250 nM for 6 hr). Then the plate was washed and the medium was replaced with pre-warmed running medium (XF base medium supplemented with 25 mM D-glucose, 1 mM pyruvate, and 2 mM glutamine for the mitochondrial stress test), followed by incubation in a non-CO₂ incubator at 37°C for 60 min. After the basal oxygen consumption rate and extracellular acidification rate were recorded for 24 min, the mitochondrial stress test was performed (1 μ M oligomycin, 2 μ M FCCP, and 0.5 μ M rotenone/ antimycin A). All reagents were from the Seahorse XF Cell Mito Stress Test Kit (Seahorse Bioscience, #103015-100). After these analyses, the number of cells in each well was counted and results were adjusted per 1x10⁵ cells.

Adeno associated virus (AAV) and IVIS imaging system

pAAV-sh-*Gabbr1* and pAAV-sh-Negative control vectors were constructed using standard subcloning techniques according to the manufacturer's instructions (AAV-DJ Helper Free shRNA Expression System, Cell Biolabs Inc, VPK-413-DJ). Annealed complementary nucleotides for shRNA target site against mouse *Gabbr1* or negative control were subcloned into BamHI/EcoRI sites of pAAV-U6-GFP expression vector. We co-transfected HEK293 cells with pAAV expression vector, pAAV-DJ and pHelper using transfection reagent (X-tremeGENE9 DNA Transfection Reagent, Roche, 06365809001). AAV was harvested from these cells by freeze and thaw cycles, and purified with a ViraBind AAV Purification Kit (Cell Biolabs Inc, VPK-140). Titer of purified AAV was quantified with QuickTiter AAV Quantitation Kit (Cell Biolabs Inc, VPK-145). We injected AAV into BAT under direct visual guidance as described previously (Shimizu et al., 2014). The titer of AAV was 1x10⁹ GC/mice. AAV injection was performed in mice (17-19 weeks age) fed HFD for more than 12 weeks since 5 weeks of age. Physiological studies were performed at postoperative days 10 to 18, and

tissues were collected for further analyses at postoperative days 21 to 22. In some studies, collected BAT was analyzed with IVIS in ex-vivo setting (IVIS lumina III, Summit Pharmaceuticals international corporation), and GFP signal was detected. Sequence of shRNA were as follows.

sh-Gabbr1

5'-GATCCGCGGTTTCCAACGTTCTTTCGAAGAGACGAAAGAACGTTGGAAACCGCTTTTTTG-3'
5'-AATTCAAAAAGCGGTTTCCAACGTTCTTTCGTCTCTTCGAAAGAACGTTGGAAACCGCG-3'

QUANTIFICATION AND STATISTICAL ANALYSIS

Statistical analyses were done with SPSS version 24 software. Data are shown as the mean \pm SEM. Differences between groups were examined by the two-tailed Student's t test or two-way ANOVA, followed by Tukey's multiple comparison test, the non-parametric Kruskal Wallis test, or Dunnett's test for comparisons among more than two groups. In all analyses, $p < 0.05$ was considered statistically significant.